

Hierarchical classification of land use types using multiple vegetation indices to measure the effects of urbanization

Sharmin Shishir  · Shiro Tsuyuzaki

Received: 30 December 2017 / Accepted: 2 May 2018 / Published online: 11 May 2018
© Springer International Publishing AG, part of Springer Nature 2018

Abstract Detecting fine-scale spatiotemporal land use changes is a prerequisite for understanding and predicting the effects of urbanization and its related human impacts on the ecosystem. Land use changes are frequently examined using vegetation indices (VIs), although the validation of these indices has not been conducted at a high resolution. Therefore, a hierarchical classification was constructed to obtain accurate land use types at a fine scale. The characteristics of four popular VIs were investigated prior to examining the hierarchical classification by using Purbachal New Town, Bangladesh, which exhibits ongoing urbanization. These four VIs are the normalized difference VI (NDVI), green-red VI (GRVI), enhanced VI (EVI), and two-band EVI (EVI2). The reflectance data were obtained by the IKONOS (0.8-m resolution) and WorldView-2 sensor (0.5-m resolution) in 2001 and 2015, respectively. The hierarchical classification of land use types was constructed using a decision tree (DT) utilizing all four of the examined VIs. The accuracy of the classification was evaluated using ground truth data with multiple comparisons and $kappa$ (κ) coefficients. The DT showed overall accuracies of 96.1 and 97.8% in 2001

and 2015, respectively, while the accuracies of the VIs were less than 91.2%. These results indicate that each VI exhibits unique advantages. In addition, the DT was the best classifier of land use types, particularly for native ecosystems represented by *Shorea* forests and home-stead vegetation, at the fine scale. Since the conservation of these native ecosystems is of prime importance, DTs based on hierarchical classifications should be used more widely.

Keywords Fine-scale data · Hierarchical classification · Decision tree · Land use change · *Shorea* forest

Introduction

Since the construction of new towns within natural ecosystems can cause the rapid deterioration of endangered and threatened ecosystems and landscape diversities therein, it is necessary to predict the effects of land use changes to promote the conservation and restoration of ecosystems prior to urbanization. Fine-resolution data are desirable for detecting land use changes as a result of urbanization; accordingly, the resolution of land use maps should be sufficiently fine for detecting the effects of road networks and of related human impacts on adjacent areas (Nigam 2000; Erner et al. 2012; Akay and Sertel 2016). However, due to the lack of high-resolution data, such detailed analyses are scarce (Fonji and Taff 2014; Kalyani and Govindarajulu 2015). Two satellites, namely, IKONOS and WorldView-2 (WV2), recently provided high-

S. Shishir (✉)
Graduate School of Environmental Science, Hokkaido University,
N-10 W-5, North Ward, Sapporo 060-0810, Japan
e-mail: s_shishir@eis.hokudai.ac.jp

S. Tsuyuzaki
Graduate School of Environmental Earth Science, Hokkaido
University, Sapporo 060-0810, Japan

resolution data with a resolution of less than 1 m (Aguilar et al. 2013). Such a resolution is likely to be suitable for analyzing land use changes caused by urbanization (Nouri et al. 2014), although the effectiveness of these datasets has not been examined. Therefore, the prime objective of the present study is to validate the applicability of these high-resolution satellite data to the detection of land use changes caused by urbanization.

The vegetation index (VI) was developed to detect the characteristics of vegetation and land use via the combination of two or more wavelength bands related to photosynthesis, i.e., the blue, green, red, and near-infrared bands (Huete et al. 1999). A high VI indicates a high vegetation greenness related to the high activities and low stresses of plants, and vice versa (Rocha and Shaver 2009). Therefore, VIs are often applied to analyses of land use and vegetation changes, e.g., to detect spatial variabilities (Matsushita et al. 2007), plant cover distributions and densities (Myneni et al. 1997; Saleska et al. 2007), and temporal changes (Lunetta et al. 2006). To evaluate the greenness of the ground surface, various VIs have been proposed (Joshi and Chandra 2011; Barzegar et al. 2015), and they are represented by the normalized difference vegetation index (NDVI), enhanced vegetation index (EVI), two-band enhanced vegetation index (EVI2), and green-red vegetation index (GRVI) (Jiang et al. 2007).

The NDVI is widely used to detect land use-land cover (LULC) changes (Sahebjalal and Dashtekian 2013; Singh et al. 2016). Additionally, measurements of the NDVI are employed to broadly assess the spatio-temporal characteristics of LULC, including the vegetation cover (Kinthada et al. 2014). The principle of the NDVI is derived from the reflectance characteristics of photosynthesis, i.e., through an examination of the vegetation greenness by using red band signals absorbed by plants and near-infrared band signals reflected by plants (Rouse et al. 1974). The weakness of this index lies in the fact that atmospheric and/or ground surface conditions, such as clouds and soils, often distort its accuracy (Kushida et al. 2015; Miura et al. 2001). Three indices, namely, the EVI, EVI2, and GRVI, were developed to reduce these obstacles, and they are popularly employed in addition to the NDVI (Phompila et al. 2015). The EVI enhances the greenness signal of the ground surface, which includes forest canopy structures, by using the blue band (Huete et al. 2002) and therefore reduces soil and atmospheric interference (Holben and Justice 1981). The EVI2 was modified from the EVI by removing the

blue band to improve the auto-correlative defects of surface reflectance spectra between the red and blue wavelengths (Jiang et al. 2008), particularly when the background soil reflectance fluctuates (Kushida et al. 2015). The GRVI is often applied to evaluate forest degradation and canopy tree phenology, because this index is sensitive to changes in the leaf color at the canopy surface by using green wavelengths (Motohka et al. 2010).

The effectiveness of each of the abovementioned VIs has been compared well at coarse scales, e.g., at 30 m with Landsat TM5 data and at 250 m with both MOD13Q1 and NOAA-AVHRR imagery (Julien et al. 2011). However, only a few studies have been conducted to investigate LULC changes using VI time series (Markogianni et al. 2013). Land use classification schemes using VIs at a fine scale should be validated prior to examining land use changes, because the accuracies of these VIs at higher resolutions have not been examined thoroughly. A new planned township, namely, Purbachal New Town, is being prepared on the northeastern side of Dhaka, Bangladesh (Rahman et al. 2016a). High-resolution data are available for a land use comparison between the pre- and post-urbanization periods. Therefore, the effectiveness of each of the four popular vegetation indices, namely, the EVI2, EVI, GRVI, and NDVI, were examined at a high resolution by comparing the two phases of urbanization (i.e., pre-urbanization and present-day) in the new township. Each VI has both strong and weak points with regard to the classification of land use types (Dibs et al. 2017). To solve this issue, a decision tree (DT) was also utilized in this study. The application of DTs has been increased for image classification purposes because of their accuracy and interpretation capabilities. DTs are effective for categorizing and selecting each class in a classification tree (Laliberte et al. 2007), and they have performed successfully with remotely sensed data for the analysis of land use changes at coarse resolutions (Brown de Colstoun et al. 2003; Sesnie et al. 2008), although their accuracy was not examined for fine resolutions (high-resolution satellite imagery < 30 m and very high-resolution ≤ 5 m) (Fisher et al. 2017).

The first objective in this study was to examine the efficiencies of the VIs with regard to land use classification at a fine scale, because their efficiencies may differ between coarse and fine resolutions. The second objective was to characterize the VIs for each land type

and to develop a hierarchical classification using a DT utilizing the characteristics of the examined VIs. Finally, the third objective was to characterize the land use changes induced by urbanization.

Materials and methods

Study area

Purbachal New Town, Bangladesh (23° 49' 45.53"–23° 52' 30.72" N and 90° 28' 20.18"–90° 32' 43.26" E) was selected as the study area (Fig. 1). At a large scale, Purbachal New Town is located within eastern-central Bangladesh between large floodplains (i.e., the Old Brahmaputra Floodplains) and terraces and is sandwiched by two rivers, namely, the Balu and

Sitalakkhya Rivers, on the west and east sides. The maximum mean monthly temperature is 26.3 °C in August, and the minimum is 12.7 °C in January (Shapla et al. 2015). The annual precipitation is 2030 mm. The dry season generally ranges from December to February, and the rainy season lasts from June to September (Rahman et al. 2016b). The new town project was established to reduce the overpopulation in the capital city of Dhaka, the population density of which was 57,167/km² in 2011 (Khatun et al. 2015). The planned area of the new town is 2489 ha (Zaman 2016). The construction started in 1995, and it did not cease until 2015. Prior to urbanization, the major land use types were forest (*Shorea robusta* Gaertner f., in the Dipterocarpaceae family, locally called *Sal* forest), homestead, homestead vegetation, cropland, and various others (Rahman et al. 2016a).

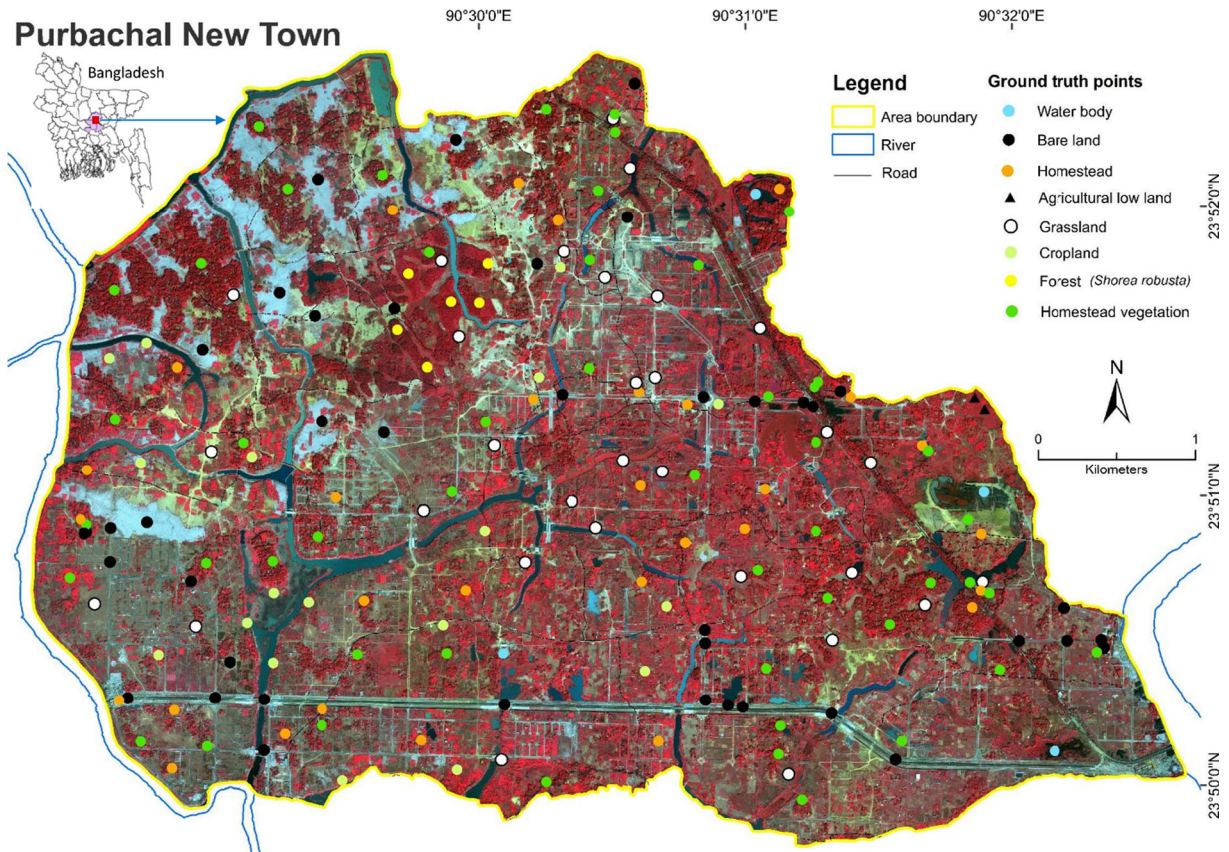


Fig. 1 Image of Purbachal New Town in 2015 from the WV2 satellite. Two rivers, namely, the Balu and Sitalakkhya Rivers, are distributed along the west and east sides of the township, respectively. The inset map at the top left shows Purbachal New Town in the country of Bangladesh. The 182 ground truth locations

recorded via GPS in Purbachal New Town are shown on the WV2 natural color image using different colored circles for different land use types. The land use types were verified to assess the accuracy of the land use classification via satellite imagery and reference vegetation maps

The expansion of urban areas in Bangladesh was inadequately planned and controlled due to truncated laws (Hossain 2013). Per the Environmental Conservation Act of 1995 and the Bangladesh Environmental Conservation Rules, 1997, the preservation of natural forests and privately owned commercial forests dominated by *Shorea robusta* should take priority during the land development planning of Purbachal New Town. The major forest products are edible fruits, timber, and medicines. These preserved forests are expected to sustain endemic and/or invaluable flora and fauna, although land development activities often neglect these perspectives (Zaman 2016). Although the emphasis during the pre-planning stage was the in situ preservation of entire forests, the idea to maintain all of the patches of *Shorea* forest was later rejected because those isolated patches had already been exposed to human activities. To compensate for the loss of forested area, a green belt with a width of 15 m to be produced through afforestation was planned for the full perimeter of the township area (24.2 km²) with a few exceptions. There were no interferences with the natural drainage systems that had maintained the pristine ecosystems in the region.

In total, the land use types of the study area were classified into eight categories (Table 4). Of those land use types, native forests with a maximum height of 36 m dominated by *Shorea robusta* have maintained the highest biodiversity, and they contain numerous endangered species (Gautam and Devoe 2006; Mandal et al. 2013). Therefore, the accurate detection of the distribution of *Shorea* forest was the priority for this land use analysis. The other land use types were homestead (i.e., settlement and residential areas), homestead vegetation (vegetation consisting of trees, shrubs and herbs on and around the settlement), cropland, grassland, agricultural low land, bare land, and water bodies. In general, therefore, homestead vegetation is larger than homestead. The homestead vegetation and agricultural low land types also support a high biodiversity (Hasnat and Hoque 2016). Currently, the forest ecosystems in the region are decreasing rapidly due to economical demands and human interferences, such as overexploitation, deforestation, excessive trash buildup, and encroachment (Salam et al. 1999; Hassan 2004). Among the artificial land use types, cropland, the major products of which are rice, jute and vegetables (e.g., cultivars consisting of gourds, beans, cabbage, cauliflower and tomatoes), was distributed broadly prior to urbanization (Shapla et al. 2015).

IKONOS and WV2 data

The data were obtained from the satellite imagery of IKONOS at 04:35 (GMT) on May 1, 2001, and at 04:44 on February 16, 2002, prior to urbanization and from WV2 imagery at 04:41 on December 9, 2015 (Digital Globe - Apollo Mapping, Longmont, Colorado, USA) at present stage, since IKONOS terminated data acquisition after 2014 and WV started data collection in October 2009. The resolutions of the IKONOS and WV2 sensors are 0.8 m (true color) and 0.5 m (natural color), respectively. All of the images were devoid of clouds.

These remote sensing data were integrated via ArcGIS (version 10.2). Integrated analyses were conducted after checking the quality of the pre-processed data to remove noise and unify the georeferences. These images were re-projected onto the Bangladesh Transverse Mercator (BTM) projection to record the statistics of landscape changes, because of the projected coordinate system in Bangladesh (Dewan and Yamaguchi 2009).

Evaluation of the vegetation indices and hierarchical classification

The categories of land use types were matched with the land use map published by the Ministry of Housing and Public Works of Bangladesh (Anonymous 2013) with a few modifications adjusted to recently developed land use patterns. The modification was made by establishing three land use types, cropland, grassland and bare land, all of which were cultivable land in the original map (Anonymous 2013). Because the map was manufactured based on various datasets consisting of topographical, geographical and historical data at a fine scale, this map was utilized as a reference during the evaluation of land use classifications.

A total of 11 VIs was investigated to confirm the accuracy of land use change detection by using error matrix prior to the construction of DT. These 11 VIs were NDVI, EVI2, EVI, GRVI, atmospherically resistant vegetation index (ARVI), green difference vegetation index (GDVI), green normalized difference vegetation index (GNDVI), difference vegetation index (DVI), normalized green (NG), ratio vegetation index (RVI) and enhanced normalized difference vegetation index (ENDVI). The four examined VIs showed higher than 65% overall accuracy, while the other VIs showed less than 50%. Therefore, the four VIs, NDVI, EVI2, EVI, and GRVI were used for the further analysis.

The four examined vegetation indices were as follows:

$$NDVI = (NIR - red) / (NIR + red) \tag{1}$$

$$GRVI = (green - red) / (green + red) \tag{2}$$

$$EVI = G \times (NIR - red) / (NIR + C_1 \times red - C_2 \times blue + L) \tag{3}$$

$$EVI2 = 2.5 \times (NIR - red) / (NIR + 2.4 \times red + 1.0), \tag{4}$$

where near-infrared (NIR), red, green and blue represent (partially) atmospherically corrected surface reflectances, L denotes the canopy background adjustment used to address the nonlinear, differential transmittance of NIR and red wavelength radiances through a canopy, and C₁ and C₂ are the coefficients of the aerosol resistance term that uses the blue band to calibrate the aerosol influences in the red wavelength. The blue wavelength ranges from 445 to 516 nm on IKONOS and from 450 to 510 nm on WV2, the green wavelength ranges from 506 to 595 nm on IKONOS and from 510 to 580 nm on WV2, the red wavelength ranges from 632 to 698 nm on IKONOS and from 630 to 690 nm on WV2, and the NIR wavelength lies between 757 and 863 nm on IKONOS and between 765 and 901 nm on WV2. Therefore, the data collected by WV2 were comparable to the data acquired using the IKONOS sensor (Table 1).

The NDVI refers to two spectral bands of the photo-synthetic output, i.e., the red and near-infrared bands (Huete et al. 1997). The NDVI ranges from -1 to +1 and increases with an increase in the vegetation greenness. However, the NDVI is skewed by background reflectances and atmospheric interference (Karnieli et al. 2013). In addition, the NDVI is saturated in regions with a high biomass (Miura et al. 2001). To reduce these disadvantages of the NDVI, multiple VIs modified from the NDVI have been developed (Phompila et al. 2015).

The GRVI uses green and red bands to assess deforestation, forest degradation and canopy tree phenology (Motohka et al. 2010; Tucker 1979). The GRVI often focuses on seasonal fluctuations in the greenness by evaluating the colors of leaves at the canopy surface using the green band (Nagai et al. 2012).

The EVI was modified from the NDVI by adopting numerous coefficients within the EVI algorithm (Eq. 3):

Table 1 The four wavelength bands on IKONOS and WV2 images

Band	Wavelength (nm)		
	IKONOS	WV2	
Blue	Min	445	450
	Max	516	510
Green	Min	506	510
	Max	595	580
Red	Min	632	630
	Max	698	690
Near-infrared (NIR)	Min	757	765
	Max	863	901

L = 1, C₁ = 6, C₂ = 7.5, and gain factor (G) = 2.5 (Rouse et al. 1974; Huete et al. 1994). These parameters are used to improve the sensitivity to high biomass regions and the vegetation monitoring capability of the EVI by dissociating the canopy background signal and diminishing atmospheric influences (Huete et al. 1999).

Although the EVI2 measures the vegetation greenness without a blue band (Eq. 4), it resembles the 3-band EVI when the data quality is high and atmospheric effects are insignificant (Jiang et al. 2008).

A DT classifier was applied to identify the land use types using the four examined VIs. The DT was implemented depending on multiple levels of decisions based on the properties of the input datasets (Mountrakis et al. 2011).

Accuracy assessment of the land use classification

Validating the land use classification is a prerequisite for confirming temporal land use changes (Foody 2002). Ground truth data of stratified land use classes at 182 locations marked with GPS were used for the validation (Fig. 1). The ground truth points were selected by using a land use map (Anonymous 2013). These locations and their adjacent areas were recorded more than once to inspect the eight land use types. Based on the measurements, the land use types on the maps were repeatedly reclassified to minimize classification errors. The accuracies of the land use classification schemes using the four VIs and of the hierarchical classification using the DT classifier were tested using an error matrix represented by an overall accuracy and a κ coefficient at each ground truth point. The ESRI ArcMap (version 10.2)

software was used for the data processing, including the statistical analysis.

Relationships between land use types and VIs

One-way analysis of variance (ANOVA) was used to investigate the significant differences in the VI values among the land use types. When the ANOVA was significant, Tukey post hoc multiple comparison tests were applied to determine the significant differences in the VIs among the land use types confirmed using ground truth data (Zar 1999).

Results

Surface reflectances in the VIs

The spatial patterns of the surface greenness in 2001 and 2015 were different among the VIs (Fig. 2). The GRVI effectively diagnosed the distributions of homestead vegetation and *Shorea* forest but often failed to discern cropland. The EVI detected the grassland distribution most correctly but could not clearly detect the *Shorea* forests. The NDVI differentiated water bodies and bare land but did not delineate the *Shorea* forest and homestead vegetation land use types, showing that the NDVI is not appropriate for classifying regions with dense green vegetation. The EVI2 distinguished vegetated land use types from non-vegetated land use types and clearly identified the homestead distribution.

The lowest NDVI value of -0.05 was obtained for water bodies due to the lack of vegetation (Fig. 3). Homestead was detected within a few small patches with a low NDVI of 0.31 in 2001 and 0.21 in 2015, confirming that a fine-scale classification is required to detect these land use types. Homestead vegetation (i.e., vegetation enclosing homesteads) showed an NDVI of 0.91 in 2001 and 0.82 in 2015. Croplands had higher a NDVI than grassland of 0.67 in 2001 and 0.59 in 2015.

The lowest EVI values were shown for water bodies, while the second-lowest values were displayed over bare land (Table 2). The EVI did not separate these two land use types clearly. The EVI of grassland was an average of 0.37, which is intermediate between the EVI values for bare land and forests. EVI values between 0.37 and 0.48 were associated with cropland and occasionally grassland, while EVI values ranging from

0.48 to 0.57 represented dense and/or deeply green vegetation.

The highest EVI2 value, i.e., 1, represented dense vegetation, including homestead vegetation. The EVI2 value for *Shorea* forest was 0.97, which was the highest of the examined VIs (0.77 with the NDVI, 0.53 with the EVI and 0.25 with the GRVI). The EVI2 value for grassland ranged from 0.10 to 0.49, which is higher than those obtained with the EVI, NDVI and GRVI. The EVI2 sometimes misclassified cropland as grassland, probably because of double cropping. An EVI2 value lower than 0.10 indicated poorly vegetated land use types, such as bare land and sparse grassland. The GRVI demonstrated an appropriate detection of densely vegetated land use types, mostly due to the discrimination of *Shorea* forest and homestead vegetation. However, the GRVI did not effectively discriminate among water bodies, bare land and homestead (Fig. 2). Non-vegetated land, i.e., water bodies and bare land, showed GRVI values of less than 0.18. Bare land and water bodies showed the lowest GRVI values of -0.04 and 0.01, respectively, while water bodies showed the lowest VI values overall. These results indicate that the GRVI performed better while distinguishing dense vegetation than other land use types characterized by sparse greenness.

In total, the NDVI had higher values than the EVI and GRVI, particularly when the reflectance was high (Fig. 3). The GRVI occasionally showed negative values over bare land when it should have been higher than 0, which was probably due to soil interference. All of the VIs showed a clear gap between non-vegetated and vegetated land use types. However, in areas with a high vegetation, the VIs exhibited different responses to greenness.

Validation of the VIs

The accuracies of the land type classification schemes were different among the VIs (Table 3). Each of the four VIs showed different values among the land use types (ANOVA, $p < 0.0001$) (Table 2). All of the VIs showed stable values over homesteads. The EVI2 and NDVI responses to grassland and cropland fluctuated, and the EVI fluctuated largely over *Shorea* forest and homestead vegetation. Although the GRVI responses to *Shorea* forest and homestead vegetation were stable, the GRVI responses were lower than the responses of the other VIs.

The EVI2 exhibited different pairs of land use types except for grassland-agricultural low land, agricultural

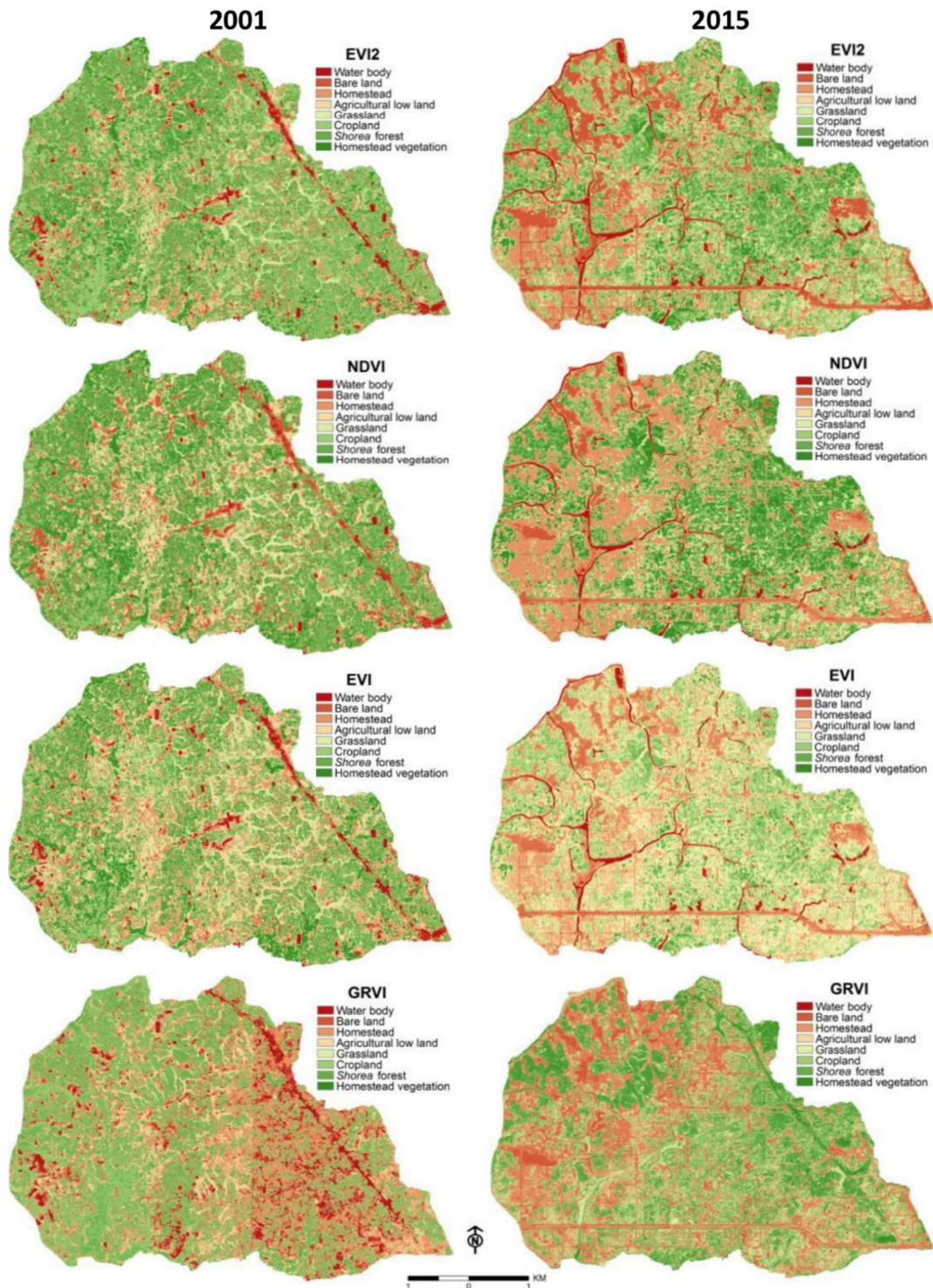


Fig. 2 Surface greenness distributions evaluated using the four VIs based on multi-temporal information from the IKONOS and WV2 images in 2001 (left side) and 2015 (right side), respectively

low land-homestead and bare land-water body (Tukey test, $p < 0.05$). The NDVI exhibited different pairs of land

use types except for homestead vegetation-Shorea forest, agricultural low land-homestead and grassland-

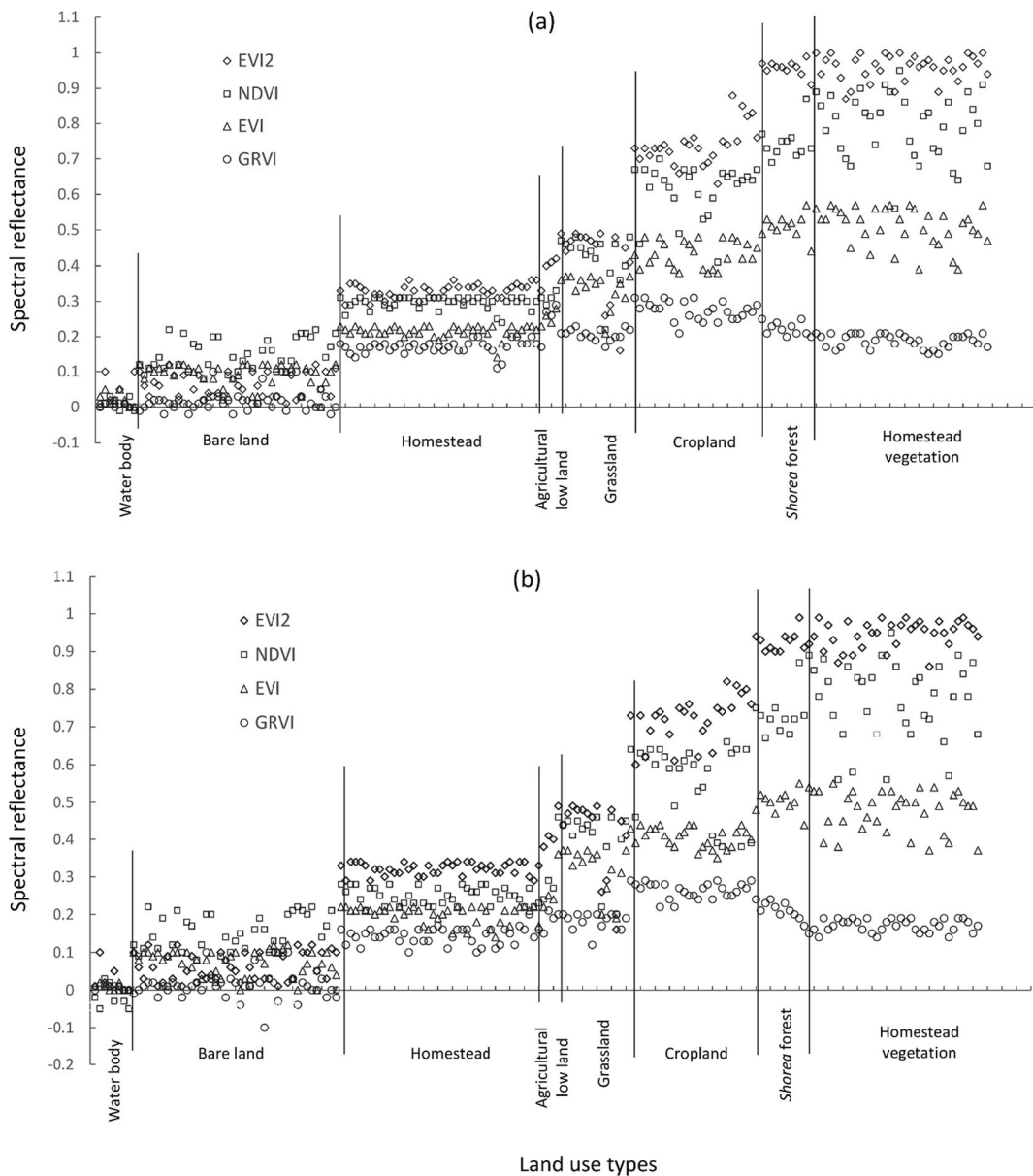


Fig. 3 Spectral reflectances in the VIs extracted from 182 ground truth points for eight land use classes. The y-axis indicates the

spectral reflectances among the four VIs, while the x-axis represents the eight land use types

agricultural low land. The homestead vegetation-*Shorea* forest and agricultural low land-homestead pairs were not significantly different in the EVI, although the rest of the pairs were different. The GRVI was capable of distinguishing between homestead vegetation and *Shorea* forest, but the other three VIs could not differentiate these two land use types. The GRVI did not reveal significant differences in the comparisons between the other land use types ($p < 0.05$). The GRVI was most effective at differentiating the *Shorea* forest-homestead vegetation pair;

meanwhile, the EVI2 and NDVI effectively detected homestead, bare land and water bodies, and the EVI effectively detected the distributions of agricultural low land, grassland and cropland.

Hierarchical classification of land use types

A hierarchical land use classification was developed using a DT classifier with the four VIs (Fig. 4).

Table 2 Mean and standard error (SE) of each VI for the eight land use types. All of the VIs obtained in 2001 and 2015 among the land use types are significantly different (one-way ANOVA,

$p < 0.0001$). Identical letters indicate that the VIs are not significantly different between those land use types (Tukey test, $p < 0.05$)

		Water body	Bare land	Homestead	Agricultural low land	Grassland	Cropland	Forest (<i>Shorea robusta</i>)	Homestead vegetation
2001	EVI2	0.04 ± 0.02 a	0.06 ± 0.01 a	0.32 ± 0.00 b	0.42 ± 0.01 c	0.42 ± 0.03 c	0.74 ± 0.01 d	0.96 ± 0.00 e	0.96 ± 0.01 e
	NDVI	0.01 ± 0.01 a	0.14 ± 0.01 b	0.30 ± 0.00 c	0.31 ± 0.01 cd	0.42 ± 0.02 d	0.62 ± 0.01 e	0.73 ± 0.01 f	0.79 ± 0.02 f
	EVI	0.02 ± 0.01 a	0.09 ± 0.01 b	0.22 ± 0.00 c	0.26 ± 0.01 c	0.34 ± 0.01 d	0.43 ± 0.01 e	0.51 ± 0.01 f	0.51 ± 0.01 f
	GRVI	0.01 ± 0.00 a	0.01 ± 0.01 a	0.17 ± 0.00 b	0.27 ± 0.01 cef	0.21 ± 0.00 dfg	0.27 ± 0.01 e	0.23 ± 0.01 f	0.19 ± 0.00 g
2015	EVI2	0.03 ± 0.01 a	0.06 ± 0.01 a	0.32 ± 0.00 b	0.40 ± 0.01 bc	0.42 ± 0.03 c	0.72 ± 0.01 d	0.92 ± 0.01 e	0.95 ± 0.01 e
	NDVI	-0.02 ± 0.01 a	0.14 ± 0.01 b	0.25 ± 0.00 c	0.27 ± 0.02 cd	0.41 ± 0.02 d	0.56 ± 0.02 e	0.71 ± 0.01 f	0.77 ± 0.02 f
	EVI	0.01 ± 0.00 a	0.08 ± 0.01 b	0.2 ± 0.00 c	0.24 ± 0.01 c	0.33 ± 0.02 d	0.41 ± 0.01 e	0.50 ± 0.01 f	0.48 ± 0.01 f
	GRVI	0.01 ± 0.00 a	0.01 ± 0.01 a	0.14 ± 0.00 b	0.18 ± 0.02 bcd	0.18 ± 0.01 ce	0.26 ± 0.00 f	0.22 ± 0.01 d	0.17 ± 0.00 e

The DT begins with the EVI2, which then separates the land use types into vegetated and non-vegetated land use types. The NDVI then separates the non-vegetated land uses into water bodies and bare land. Meanwhile, among the vegetated land use types, the EVI2 extracts the homestead distribution and the EVI detects agricultural low land, grassland and cropland. Among the four VIs, homestead vegetation and *Shorea* forest were separated only through the GRVI.

The DT approach showed the highest accuracy (with an accuracy greater than 95% and a κ of greater than 0.95, see Table 3) during the land use classification, indicating that the DT constructed using the four VIs was the most effective at predicting the land use types

(Fig. 5). The second-highest accuracy and κ values (91.2% and 0.89, respectively) were exhibited by the EVI2 measurements from 2015, indicating that the DT effectively improved the land use classification scheme.

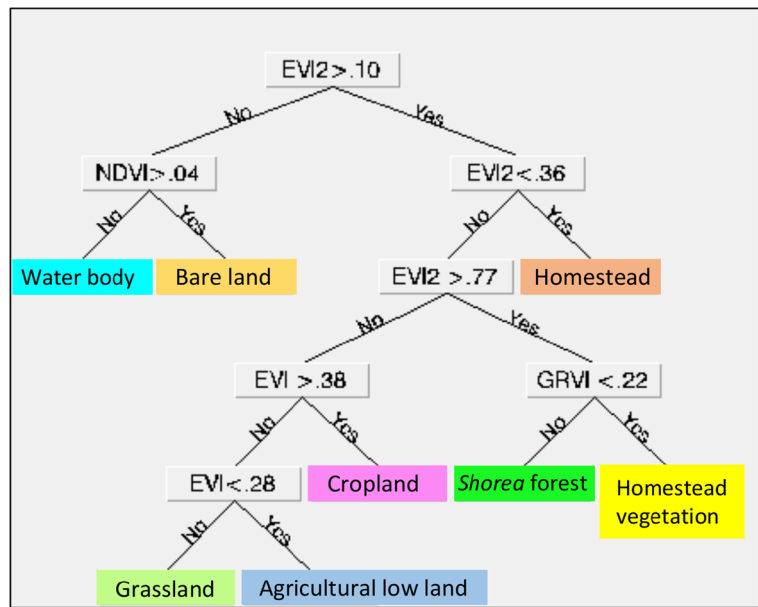
LULC changes

Based on the land use changes from 2001 to 2015 (Fig. 5), the characteristics of the land use changes were examined (Table 4). Road networks and their adjacent areas were clearly observed. Homestead vegetation, grassland, cropland and homestead were the dominant land use types prior to urbanization, but more than three-quarters of the area of each land use type was lost

Table 3 Classification accuracies examined using an error matrix of κ coefficients

Classification	2001		2015	
	Overall accuracy (%)	κ coefficient	Overall accuracy (%)	κ coefficient
EVI2	90.1	0.88	91.2	0.89
NDVI	88.5	0.86	89.6	0.87
EVI	66.5	0.60	67.6	0.61
GRVI	74.2	0.69	77.5	0.73
DT	96.1	0.95	97.8	0.97

Fig. 4 A DT constructed using the hierarchical classification of land use types. Numerals with inequality signs indicate the VI values that represent the thresholds of the classifiers



thereafter. Approximately one-half of the area of *Shorea* forest was lost subsequent to urbanization. Since the distribution of bare land increased greatly, the reduction in the area of each land use type can be derived according to an increase in bare land originating from road construction and other related construction projects, and the water body area was also increased due to the excavation of artificial lakes and canals. Grasses colonized in the filed up agricultural low land and consequently, the grassland increased. Since most of the water bodies were small and/or narrow, those changes were detectable only at a high resolution.

Discussion

Effectiveness of the VIs and the DT approach

A comparison among the DT and VIs indicates that all four of the examined VIs showed specific advantages and disadvantages with regard to the land use classification at a fine resolution. The reflectances of the blue and green wavelengths can characterize the spatiotemporal fluctuation patterns of VIs (Huete 1988). The EVI2 differentiated between vegetated and non-vegetated land use types without using the blue band. Only the GRVI classified dense vegetation, i.e., homestead vegetation and *Shorea* forests, probably because the GRVI is sensitive to the canopy surfaces of forests

(Nagai et al. 2012). Therefore, the GRVI constituted a prerequisite for the classification of deeply green areas, i.e., forests, although the overall accuracy of the associated classification was low.

The EVI2 showed the highest accuracy among the examined VIs at a fine resolution (Kushida et al. 2015). However, the EVI2 did not effectively differentiate between homestead vegetation and *Shorea* forest. The EVI2 maintains a high sensitivity and linearity to high phytomass densities (Rocha and Shaver 2009). However, there are many difficulties when using the EVI2 to conduct a land use classification in tropical/sub-tropical regions such as Bangladesh, because persistent evergreen forests show high reflectances both in and out of season (Cristiano et al. 2014). The accuracy of the NDVI land classification was slightly lower than that of the EVI2 results. The NDVI is skewed by the background reflectance, including those of bright soils and non-photosynthetic plant organs (i.e., trash and tree trunks) (Van Leeuwen and Huete 1996). Because the examined data did not contain a substantial amount of clouds, the EVI2 and NDVI seemed to synchronize their fluctuations.

The EVI effectively classified the grassland, cropland and agricultural low land types, but it did not distinguish the other land use types, suggesting that the blue band used only by the EVI influenced the resulting land use classification. However, the EVI is distorted by the soil adjustment factor L in Eq. (3), making it more sensitive

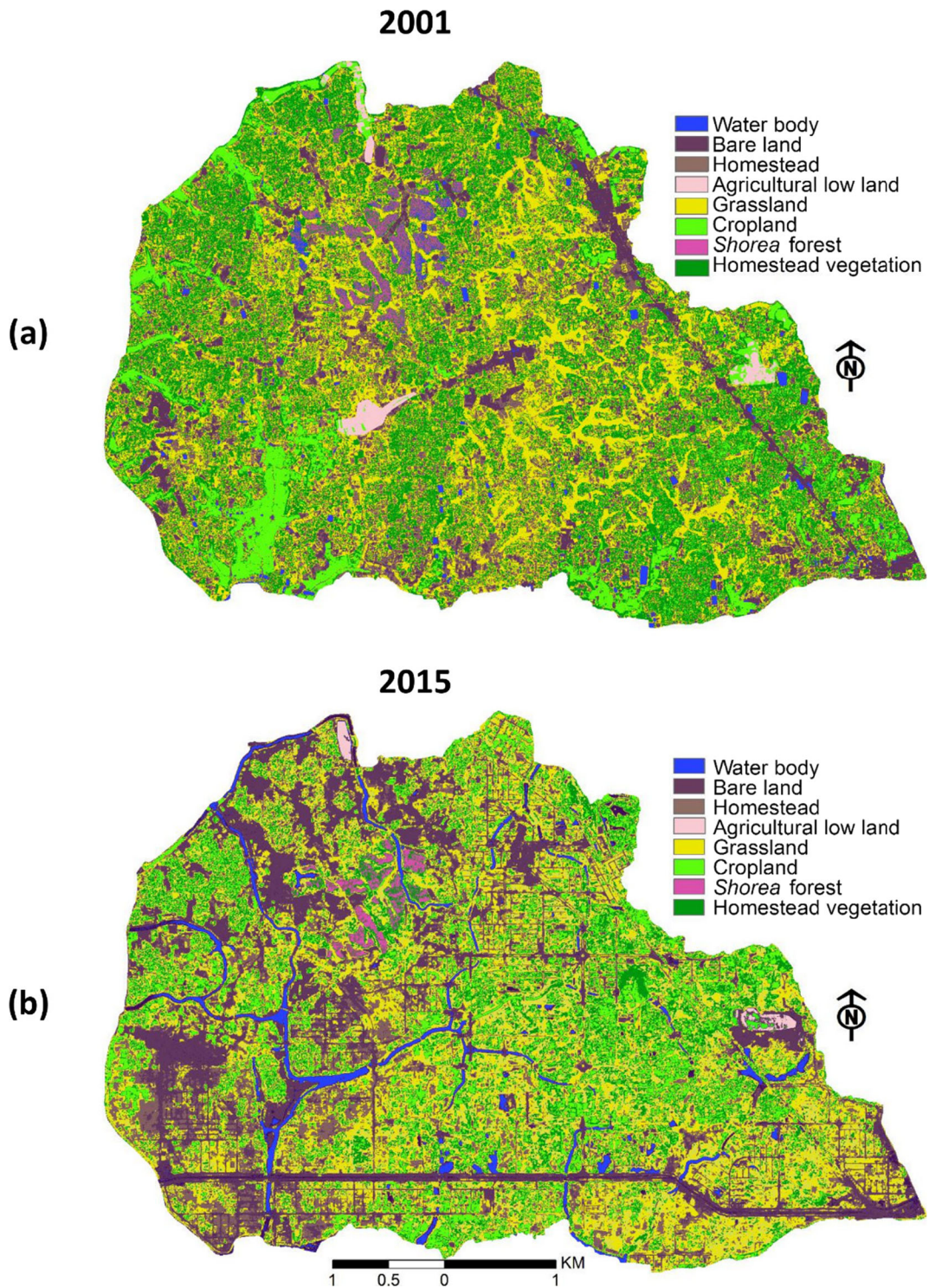


Fig. 5 Land use maps produced through a hierarchical classification using the DT approach. These maps show the temporal changes in the land use-land cover throughout Purbachal New Town from 2001 to 2015. **a** Land use patterns detected using the

IKONOS sensor in 2001. The land use patterns were verified using a pre-project land use map (Anonymous 2013). **b** Land use patterns in 2015 were detected using WV2 multi-spectral imagery. The land use types are represented by their respective colors

Table 4 Changes in the eight land use types from 2001 to 2015 based on satellite imagery

Land use types	2001		2015	
	Area (km ²)	(%)	Area (km ²)	(%)
Water body	0.59	2.37	2.12	8.52
Bare land	0.14	0.56	16.97	68.17
Homestead	3.02	12.13	0.86	3.46
Agricultural low land	0.67	2.69	0.04	0.16
Grassland	1.03	4.14	1.06	4.26
Cropland	6.26	25.15	0.59	2.37
Forest (<i>Shorea robusta</i>)	0.77	3.09	0.42	1.69
Homestead vegetation	12.41	49.86	2.83	11.37

to topographic conditions (Wardlow et al. 2007). Therefore, the EVI did not seem to function well.

The DT using the four VIs largely improved the accuracy of the land use classification. The accuracy of the DT was slightly different between the two surveyed years (96.1% in 2001 and 97.8% in 2015, see Table 3). One cause of this difference was probably derived from differences in the quality of the data, i.e., with regard to the resolution, photographing conditions and sensors, from IKONOS in 2001 and from WV2 in 2015.

Temporal land use changes caused by urbanization

This research used highly resolved, multi-temporal satellite data to develop a methodology for assessing land use changes. The results of the VIs vary between fine and coarse resolution. The fine-scale land use classification scheme clearly detected fine-scale land use patches generated by the development of road networks subsequent to urbanization that cannot be detected during coarse-scale analysis. Accordingly, land use classification schemes are often dependent upon the resolution (O'Connell et al. 2013). Since roadways are a few tens of meters wide, high-resolution data are required for the classification of urban landscapes. Fine-scale data can delineate land cover classes more accurately, because such data can identify small and/or linear patches while retaining their shapes (Boyle et al. 2014). Ongoing urbanization has been followed by drastic changes in the land use types, biodiversity and fragile ecosystems of urbanized areas (Merlotto et al. 2012; Zhou and Zhao 2013; Pigeon et al. 2006). The urbanization of Purbachal New Town was characterized by a substantial loss of homestead vegetation and cultivable land. Furthermore, approximately one-half of native *Shorea* forests were

lost, even though the master plan of urbanization considered their conservation (Hasnat and Hoque 2016). Land use changes associated with deforestation have not been detected well. The endangered *Shorea* forests are likely to be restored and conserved through the identification of small and isolated patches using the fine-scale analysis. The species distribution modeling should be executed for the restoration of the threatened ecosystems using the identified distinct small patches. Also, land transformation model would be implemented using fine-scale data to show the process of land use changes (Pijanowski et al. 2002). These approaches are the pronounced concern for the planners to protect and preserve the endangered ecosystems from being extinction.

Imagery acquired by two or more satellites is often used to examine temporal land use changes depending on the data availability. This study used two sets of satellite imagery, namely, from the IKONOS and WV2 sensors. Using multiple sensors can often cause errors in the land use classification due to heterogeneities in the spatial resolution of the data (Joshi et al. 2016; Xie et al. 2008). However, integrating the IKONOS and WV2 data resulted in a smaller error and higher accuracy; this was probably because of the finer resolutions and greater overlap of the wavelength bands. Fine-resolution data may partly resolve such errors by reducing the mismatches in the overlays of wavelength bands.

Conclusion

A DT constructed using a hierarchical classification greatly improved the classification of land use types at a fine resolution. The DT was developed using all of the four examined VIs because each VI demonstrated

unique strengths and limitations. For example, the GRVI showed the lowest overall accuracy, but it was retained in the DT because the GRVI can effectively classify areas with a high greenness. The land use classification scheme using the DT clarified that the changes in Purbachal New Town are characterized by the effects of road networks on deeply green ecosystems, which are unlikely to be detected clearly at coarse resolutions. Therefore, this research showed a significant monitoring source to investigate the continuous changes in land use types and assist the planners and decision makers to develop land use management plans.

Acknowledgements We would like to acknowledge the Japan Science Society (research number: 29-508) for providing the funding for this research. We thank Lea Vegh for her help during the satellite data acquisition and Dr. TaeOh Kwon. We are also grateful to Springer Nature Author Services for English language editing.

References

- Aguilar, M. A., Saldaña, M. M., & Aguilar, F. J. (2013). GeoEye-1 and WorldView-2 pan-sharpened imagery for object-based classification in urban environments. *International Journal of Remote Sensing*, *34*, 2583–2606. <https://doi.org/10.1080/01431161.2012.747018>.
- Akay, S. S., & Sertel, E. (2016). Urban land cover/use change detection using high resolution spot 5 and spot 6 images and urban atlas nomenclature. *The International Archives of the Photogrammetry, Remote Sensing and Spatial Information Sciences*, XLII-B8, 789–796. XXIII ISPRS Congress, Prague, Czech Republic. <https://doi.org/10.5194/isprs-archives-XLII-B8-789-2016>.
- Anonymous (2013). Environmental impact assessment (EIA) of Purbachal New Town project. Rajdhani Unnayan Kartripakkha (RAJUK), Ministry of Housing and Public Works, Government of the People's Republic of Bangladesh.
- Barzegar, M., Ebadi, H., & Kiani, A. (2015). Comparison of different vegetation indices for very high-resolution images, specific case UltraCam-D imagery. *Remote Sensing and Spatial Information Sciences*, XL-1/W5, 97–104. <https://doi.org/10.5194/isprsarchives-XL-1-W5-97-2015>.
- Boyle, S. A., Kennedy, C. M., Torres, J., Colman, K., Pérez-Estigarribia, P. E., & de la Sancha, N. U. (2014). High-resolution satellite imagery is an important yet underutilized resource in conservation biology. *PLoS One*, *9*, e86908. <https://doi.org/10.1371/journal.pone.0086908>.
- Brown De Colstoun, E. C. B., Story, M. H., Thompson, C., Commisso, K., Smith, T. G., & Irons, J. R. (2003). National Park vegetation mapping using multi-temporal Landsat 7 data and a decision tree classifier. *Remote Sensing of Environment*, *85*, 316–327.
- Cristiano, P. M., Madanes, N., Campanello, P. I., di Francescantonio, D., Rodríguez, S. A., Zhang, Y.-J., Carrasco, L. O., & Goldstein, G. (2014). High NDVI and potential canopy photosynthesis of South American subtropical forests despite seasonal changes in leaf area index and air temperature. *Forests*, *5*, 287–308. <https://doi.org/10.3390/f5020287>.
- Dewan, A. M., & Yamaguchi, Y. (2009). Using remote sensing and GIS to detect and monitor land use and land cover change in Dhaka Metropolitan of Bangladesh during 1960–2005. *Environmental Monitoring and Assessment*, *150*, 237–249. <https://doi.org/10.1007/s10661-008-0226-5>.
- Dibs, H., Idrees, M. O., & Alsalhin, G. B. A. (2017). Hierarchical classification approach for mapping rubber tree growth using per-pixel and object-oriented classifiers with SPOT-5 imagery. *The Egyptian Journal of Remote Sensing and Space Sciences*, *20*, 21–30. <https://doi.org/10.1016/j.ejrs.2017.01.004>.
- Erener, A., Düzgün, S., & Yalciner, A. C. (2012). Evaluating land use/cover change with temporal satellite data and information systems. *Procedia Technology*, *1*, 385–389. <https://doi.org/10.1016/j.protcy.2012.02.079>.
- Fisher, J. R. B., Acosta, E. A., Dennedy-Frank, P. J., Kroeger, T., & Boucher, T. M. (2017). Impact of satellite imagery spatial resolution on land use classification accuracy and modeled water quality. *Remote Sensing in Ecology and Conservation*, *n/a*, 1–13. <https://doi.org/10.1002/rse2.61>.
- Fonji, S. F., & Taff, G. N. (2014). Using satellite data to monitor land-use land-cover change in North-Eastern Latvia. *Springer Plus*, *3*, 61. <https://doi.org/10.1186/2193-1801-3-61>.
- Foody, G. M. (2002). Status of land cover classification accuracy assessment. *Remote Sensing of Environment*, *80*, 185–201. [https://doi.org/10.1016/S0034-4257\(01\)00295-4](https://doi.org/10.1016/S0034-4257(01)00295-4).
- Gautam, K. H., & Devoe, N. N. (2006). Ecological and anthropogenic niches of sal (*Shorea robusta* Gaertn. f.) forest and prospects for multiple-product forest management—a review. *Forestry (London)*, *79*, 81–101. <https://doi.org/10.1093/forestry/cpi063>.
- Hasnat, M. M., & Hoque, M. S. (2016). Developing satellite towns: a solution to housing problem or creation of new problems. *IACSIT International Journal of Engineering and Technology*, *8*, 50–56.
- Hassan, M. M. (2004). A study on flora species diversity and their relations with farmers' socio-agro-economic condition in Madhupur Sal forest. Dissertation, Department of Agroforestry, Bangladesh Agricultural University, Mymensingh.
- Holben, B. N., & Justice, C. O. (1981). An examination of spectral band ratioing to reduce the topographic effect on remotely sensed data. *International Journal of Remote Sensing*, *2*, 115–133. <https://doi.org/10.1080/01431168108948349>.
- Hossain, S. (2013). Migration, urbanization and poverty in Dhaka, Bangladesh. *Journal of the Asiatic Society of Bangladesh (Hum.)*, *58*, 369–382.
- Huete, A. (1988). A soil-adjusted vegetation index (SAVI). *Remote Sensing of Environment*, *25*, 295–309.
- Huete, A., Justice, C., & Liu, H. (1994). Development of vegetation and soil indices for MODIS-EOS. *Remote Sensing of Environment*, *49*, 224–234.
- Huete, A. R., Liu, H. Q., Batchily, K., & van Leeuwen, W. (1997). A comparison of vegetation indices over a global set of TM images for EOS-MODIS. *Remote Sensing of Environment*, *59*, 440–451. [https://doi.org/10.1016/S0034-4257\(96\)00112-5](https://doi.org/10.1016/S0034-4257(96)00112-5).

- Huete, A. R., Justice, C., & van Leeuwen, W. (1999). MODIS vegetation index (MOD13) algorithm theoretical basis document. Version 3.1. Vegetation Index and Phenology Lab, The University of Arizona.
- Huete, A., Didan, K., Miura, T., Rodriguez, E. P., Gao, X., & Ferreira, L. G. (2002). Overview of the radiometric and biophysical performance of the MODIS vegetation indices. *Remote Sensing of Environment*, *83*, 195–213. [https://doi.org/10.1016/S0034-4257\(02\)00096-2](https://doi.org/10.1016/S0034-4257(02)00096-2).
- Jiang, Z., Huete, A. R., Kim, Y., & Didan, K. (2007). 2-band enhanced vegetation index without a blue band and its application to AVHRR data. *Remote Sensing and Modeling of Ecosystems for Sustainability*, *6679(667905)*, 1–9. <https://doi.org/10.1117/12.734933>.
- Jiang, Z., Huete, A. R., Didan, K., & Miura, T. (2008). Development of a two-band enhanced vegetation index without a blue band. *Remote Sensing of Environment*, *112*, 3833–3845.
- Joshi, & Chandra, P. (2011). Performance evaluation of vegetation indices using remotely sensed data. *International Journal of Geomatics and Geosciences*, *2*, 231–240 ISSN 0976 – 4380.
- Joshi, N., Baumann, M., Ehammer, A., Fensholt, R., Grogan, K., Hostert, P., Jepsen, M. R., et al. (2016). A review of the application of optical and radar remote sensing data fusion to land use mapping and monitoring. *Remote Sensing*, *8*, 70. <https://doi.org/10.3390/rs8010070>.
- Julien, Y., Sobrino, J. A., Mattar, C., Ruescas, A. B., Jime'nez-Munoz, J. C., So'ria, G., Hidalgo, V., Atitar, M., Franch, B., & Cuenca, J. (2011). Temporal analysis of normalized difference vegetation index (NDVI) and land surface temperature (LST) parameters to detect changes in the Iberian land cover between 1981 and 2001. *International Journal of Remote Sensing*, *32*, 2057–2068. <https://doi.org/10.1080/01431161003762363>.
- Kalyani, P., & Govindarajulu, P. (2015). Multi-scale urban analysis using remote sensing and GIS. *Geoinformatica: An International Journal (GIIJ)*, *5*, 1–11.
- Karnieli, A., Bayarjargal, Y., Bayasgalan, M., Mandakh, B., Dugarjav, C., Burgheimer, J., Khudulmur, S., Bazha, S. N., & Gunin, P. D. (2013). Do vegetation indices provide a reliable indication of vegetation degradation? A case study in the Mongolian pastures. *International Journal of Remote Sensing*, *34*, 6243–6262. <https://doi.org/10.1080/01431161.2013.793865>.
- Khatun, H., Falgune, N., & Kutub, M. J. R. (2015). Analyzing urban population density gradient of Dhaka metropolitan area using geographic information systems (GIS) and census data. *Malaysian Journal of Society and Space*, *13*, 1–13 ISSN 2180-2491.
- Kinthada, N. R., Gurram, M. K., Eadara, A., & Velagala, V. R. (2014). Land use/land cover and NDVI analysis for monitoring the health of micro-watersheds of Sarada River basin, Visakhapatnam District, India. *Journal of Geology and Geophysics*, *3*, 146. <https://doi.org/10.4172/2329-6755.1000146>.
- Kushida, K., Hobara, S., Tsuyuzaki, S., Kim, Y., Watanabe, M., Setiawan, Y., Harada, K., Shaver, G. R., & Fukuda, M. (2015). Spectral indices for remote sensing of phytomass, deciduous shrubs, and productivity in Alaskan Arctic tundra. *International Journal of Remote Sensing*, *36*, 4344–4362. <https://doi.org/10.1080/01431161.2015.1080878>.
- Laliberte, A. S., Fredrickson, E. L., & Rango, A. (2007). Combining decision trees with hierarchical object-oriented image analysis for mapping arid rangelands. *Journal of Photogrammetric Engineering and Remote Sensing*, *73*, 197–207.
- Lunetta, R. S., Knight, J. F., Ediriwickrema, J., Lyon, J. G., & Worthy, L. D. (2006). Land-cover change detection using multi-temporal MODIS NDVI data. *Remote Sensing of Environment*, *105*, 142–154.
- Mandal, R. A., Yadav, B. K. V., Yadav, K. K., Dutta, I. C., & Haque, S. M. (2013). Biodiversity comparison of natural *Shorea robusta* mixed forest with *Eucalyptus Camaldulensis* plantation in Nepal. *Scholars Academic Journal of Biosciences (SAJB)*, *1*, 144–149.
- Markogianni, V., Dimitriou, E., & Kalivas, D. P. (2013). Land-use and vegetation change detection in Plastira artificial lake catchment (Greece) by using remote sensing and GIS techniques. *International Journal of Remote Sensing*, *34*, 1265–1281. <https://doi.org/10.1080/01431161.2012.718454>.
- Matsushita, B., Yang, W., Chen, J., Onda, Y., & Qiu, G. (2007). Sensitivity of the enhanced vegetation index (EVI) and normalized difference vegetation index (NDVI) to topographic effects: a case study in high-density cypress forest. *Sensors*, *7*, 2636–2651.
- Merlotto, A., Piccolo, M. C., & Bertola, G. R. (2012). Urban growth and land use/cover change at Necochea and Quequen cities, Buenos Aires province, Argentina. *Revista de Geografia Norte Grande*, *53*, 159–176.
- Miura, T., Huete, A. R., Yoshioka, H., & Holben, B. N. (2001). An error and sensitivity analysis of atmospheric resistant vegetation indices de-rived from dark target-based atmospheric correction. *Remote Sensing of Environment*, *78*, 284–298.
- Motohka, T., Nasahara, K. N., Oguma, H., & Tsuchida, S. (2010). Applicability of green-red vegetation index for remote sensing of vegetation phenology. *Remote Sensing*, *2*, 2369–2387. <https://doi.org/10.3390/rs2102369>.
- Mountrakis, G., Im, J., & Ogole, C. (2011). Support vector machines in remote sensing: a review. *ISPRS Journal of Photogrammetry and Remote Sensing*, *66(3)*, 247–259.
- Myneni, R. B., Keeling, C. D., Tucker, C. J., Asrar, G., & Nemani, R. R. (1997). Increased plant growth in the northern high latitudes from 1981 to 1991. *Nature*, *386*, 698–702. <https://doi.org/10.1038/386698a0>.
- Nagai, S., Saitoh, T. M., Kobayashi, H., Ishihara, M., Suzuki, R., Motohka, T., Nasahara, K. N., & Muraoka, H. (2012). In situ examination of the relationship between various vegetation indices and canopy phenology in an evergreen coniferous forest, Japan. *International Journal of Remote Sensing*, *33*, 6202–6214.
- Nigam, R. K. (2000). Application of remote sensing and geographical information system for land use/land cover mapping and change detection in the rural urban fringe area of Enschede City, the Netherlands. *International Archives of Photogrammetry and Remote Sensing*, *33*, 993–998.
- Nouri, H., Beecham, S., Anderson, S., & Nagler, P. (2014). High spatial resolution WorldView-2 imagery for mapping NDVI and its relationship to temporal urban landscape evapotranspiration factors. *Remote Sensing*, *6*, 580–602. <https://doi.org/10.3390/rs6010580>.
- O'Connell, J., Connolly, J., Vermote, E. F., & Holden, N. M. (2013). Radiometric normalization for change detection in peatlands: a modified temporal invariant cluster approach.

- International Journal of Remote Sensing*, 34, 2905–2924. <https://doi.org/10.1080/01431161.2012.752886>.
- Phompila, C., Lewis, M., Ostendorf, B., & Clarke, K. (2015). MODIS EVI and LST temporal response for discrimination of tropical land covers. *Remote Sensing*, 7, 6026–6040. <https://doi.org/10.3390/rs70506026>.
- Pigeon, G., Lemonsu, A., Long, N., Barrié, J., Masson, V., & Durand, P. (2006). Urban thermodynamic island in a coastal city analysed from an optimized surface network. *Boundary-Layer Meteorology*, 120, 315–351.
- Pijanowski, B. C., Brown, D. G., Shellito, B., & Manik, G. (2002). Using neural networks and GIS to forecast land use changes: a land transformation model. *Computers, Environment and Urban Systems*, 26, 553–575. [https://doi.org/10.1016/S0198-9715\(01\)00015-1](https://doi.org/10.1016/S0198-9715(01)00015-1).
- Rahman, M. A., Woobaidullah, A. S. M., Quamruzzaman, C., Rahman, M. M., Khan, A. U., & Mustahid, F. (2016a). Probable liquefaction map for Purbachal New Town, Dhaka, Bangladesh. *International Journal of Emerging Technology and Advanced Engineering*, 6, 345–356.
- Rahman, M. A., Mostafa Kamal, S. M., & Maruf Billah, M. (2016b). Rainfall variability and linear trend models on north-west part of Bangladesh for the last 40 years. *American Journal of Applied Mathematics*, 4, 158–162. <https://doi.org/10.11648/j.ajam.20160403.16>.
- Rocha, A. V., & Shaver, G. R. (2009). Advantages of a two band EVI calculated from solar and photosynthetically active radiation fluxes. *Agricultural and Forest Meteorology*, 149, 1560–1563.
- Rouse, J. W., Haas, R. H., Deering, D. W., Schell, J. A., & Harlan, J. C. (1974). Monitoring the vernal advancement and retrogradation (green wave effect) of natural vegetation. Technical Report, No E74–10676, NASA-CR-139243, PR-7. ID: 19740022555. Texas A&M Univ.; Remote Sensing Center, College Station.
- Sahebjalal, E., & Dashtekian, K. (2013). Analysis of land use-land covers changes using normalized difference vegetation index (NDVI) differencing and classification methods. *African Journal of Agricultural Research*, 8, 4614–4622. <https://doi.org/10.5897/AJAR11.1825>.
- Salam, M. A., Noguchi, T., & Koike, M. (1999). The causes of forest cover loss in the hill forests in Bangladesh. *GeoJournal*, 47, 539–549.
- Saleska, S. R., Didan, K., Huete, A. R., & da Rocha, H. R. (2007). Amazon forests green-up during 2005 drought. *Science*, 318, 612.
- Sesnie, S. E., Gessler, P. E., Finegan, B., & Thessler, S. (2008). Integrating Landsat TM and SRTM-DEM derived variables with decision trees for habitat classification and change detection in complex neotropical environments. *Remote Sensing of Environment*, 112(5), 2145–2159.
- Shapla, T., Park, J., Hongo, C., & Kuze, H. (2015). Agricultural land cover change in Gazipur, Bangladesh, in relation to local economy studied using Landsat images. *Advances in Remote Sensing*, 4, 214–223. <https://doi.org/10.4236/ars.2015.43017>.
- Singh, R. P., Singh, N., Singh, S., & Mukherjee, S. (2016). Normalized difference vegetation index (NDVI) based classification to assess the change in land use/land cover (LULC) in Lower Assam, India. *International Journal of Advanced Remote Sensing and GIS*, 5, 1963–1970. <https://doi.org/10.23953/cloud.ijarsg.74>.
- Tucker, C. J. (1979). Red and photographic infrared linear combinations for monitoring vegetation. *Remote Sensing of Environment*, 8, 127–150. [https://doi.org/10.1016/0034-4257\(79\)90013-0](https://doi.org/10.1016/0034-4257(79)90013-0).
- Van Leeuwen, W. J. D., & Huete, A. R. (1996). Effects of standing litter on the biophysical interpretation of plant canopies with spectral indices. *Remote Sensing of Environment*, 55, 123–138. [https://doi.org/10.1016/0034-4257\(95\)00198-0](https://doi.org/10.1016/0034-4257(95)00198-0).
- Wardlow, B. D., Egbert, S. L., & Kastens, J. H. (2007). Analysis of time-series MODIS 250 m vegetation index data for crop classification in the U.S. Central Great Plains. *Remote Sensing of Environment*, 108, 290–310.
- Xie, Y., Sha, Z., & Yu, M. (2008). Remote sensing imagery in vegetation mapping: a review. *Journal of Plant Ecology*, 1, 9–23. <https://doi.org/10.1093/jpe/rtm005>.
- Zaman, A. K. M. A. (2016). Precarious periphery: *Satellite township development causing socio-political economic and environmental threats at the fringe areas of Dhaka*. Unpublished Paper. Department of Architecture, KU Leuven. <https://doi.org/10.13140/rg.2.2.30067.32807>.
- Zar, J. H. (1999). *Biostatistical analysis*. Department of Biological Sciences, Northern Illinois University. 4th Ed. New Jersey 07458, USA. Prentice Hall, Inc. Simon & Schuster. ISBN 0-13-082390-2.
- Zhou, N. Q., & Zhao, S. (2013). Urbanization process and induced environmental geological hazards in China. *Natural Hazards*, 67, 797–810. <https://doi.org/10.1007/s11069-013-0606-1>.